

A Photostable AIE Luminogen for Specific Mitochondrial Imaging and Tracking

Chris Wai Tung Leung,^{†,‡} Yuning Hong,^{†,‡} Sijie Chen,[†] Engui Zhao,[†] Jacky Wing Yip Lam,[†] and Ben Zhong Tang^{*,†,‡}

[†]Department of Chemistry, Institute for Advanced Study, Division of Biomedical Engineering, State Key Laboratory of Molecular Neuroscience and Institute of Molecular Functional Materials, The Hong Kong University of Science and Technology, Clear Water Bay, Kowloon, Hong Kong, China

[‡]Guangdong Innovative Research Team, SCUT-HKUST Joint Research Laboratory, State Key Laboratory of Luminescent Materials and Devices, South China University of Technology, Guangzhou 510640, China

S Supporting Information

ABSTRACT: Tracking the dynamics of mitochondrial morphology has attracted much research interest because of its involvement in early stage apoptosis and degenerative conditions. To follow this process, highly specific and photostable fluorescent probes are in demand. Commercially available mitochondria trackers, however, suffer from poor photostability. To overcome this limitation, we have designed and synthesized a fluorescent agent, tetraphenylethene-triphenylphosphonium (TPE-TPP), for mitochondrial imaging. Inherent from the mitochondrial-targeting ability of TPP groups and the aggregation-induced emission (AIE) characteristics of the TPE core, TPE-TPP possesses high specificity to mitochondria, superior photostability, and appreciable tolerance to environmental change, allowing imaging and tracking of the mitochondrial morphological changes in a long period of time.

Mitochondria, the organelle found in almost all eukaryotic cells, play a vital role in the life and death of cells.¹ The most prominent function of mitochondria is to produce ATP, the energy currency of the cell. The production of ATP involves a series of electron-transport systems in the oxidation–phosphorylation pathway, which is also found to be associated with the generation of reactive oxygen species (ROS).^{1,2} The production of ROS in mitochondria leads to the propagation of free radicals and damaging cells and contributes to cell death, which is known as mitochondria-mediated apoptosis.^{3,4} The morphology of mitochondria, though varies upon cell type, cell-cycle stage, and intracellular metabolic state, is affected by and thus reflects cell functioning.⁵ The morphology is controlled by a set of proteins, mutations of which will cause several human diseases including degenerative diseases, such as Parkinson's and Alzheimer's diseases.⁶ Recent reports also show that proteins participating in apoptosis can affect the morphology of mitochondria.^{7,8} Tracking the mitochondrial morphological change may give insight for studying apoptosis and degenerative conditions.

Fluorescent probes that can selectively illuminate cellular mitochondria are powerful tools for monitoring the morphological changes and studying these processes. For observing the

dynamic changes in a certain period of time, the probe must be photostable under the continual irradiation of light from fluorescent microscopes. Conventional fluorescent dyes for mitochondria staining have been developed.^{9,10} Their photostability, however, leaves much to be desired. Very diluted solutions of these dyes are used in the imaging process, and such small numbers of dye molecules can be quickly photobleached when a harsh laser beam is used as the excitation light source. The photostability cannot be improved by using higher fluorophore concentration due to the accompanying concentration-quenching effect.

Luminogens with aggregation-induced emission (AIE) characteristics exhibit opposite phenomena: They are almost nonfluorescent when molecularly dissolved but become highly emissive in the aggregate state with fluorescence increasing along with the increase of fluorophore concentration.¹¹ Restriction of intramolecular motions (RIM) is proposed as the main cause of the AIE effect.¹² Lipophilic AIE molecules form nanoaggregates in aqueous solution spontaneously because of their hydrophobic nature.¹³ These nanoaggregates have been successfully applied for long-term cell tracking in our previous work.¹⁴ It is envisaged that the nanoaggregates of the AIE molecules would possess better photostability than single fluorescent molecule in dilute solutions.

To achieve the specificity to mitochondria, AIE luminogens are decorated with mitochondria targeting moieties. In this study, tetraphenylethene (TPE), an archetypal AIE luminogen, was synthesized and functionalized with triphenylphosphonium (TPP) groups (TPE-TPP, Figure 1). TPP is a well-known functional group that facilitates the entrance of molecular probes into mitochondria by its lipophilicity and electrophoretic force.² We here demonstrate that TPE-TPP can light up mitochondria specifically in live cells with superior photostability, enabling the observation of mitochondrial morphological changes.

TPE-TPP was prepared by the synthetic route, as shown in Scheme S1. The TPE core (Figure 1, TPE-TPP, blue) was synthesized simply from a McMurry coupling reaction. TPP (Figure 1, TPE-TPP, red) was attached through bromination

Received: October 24, 2012

Published: December 17, 2012

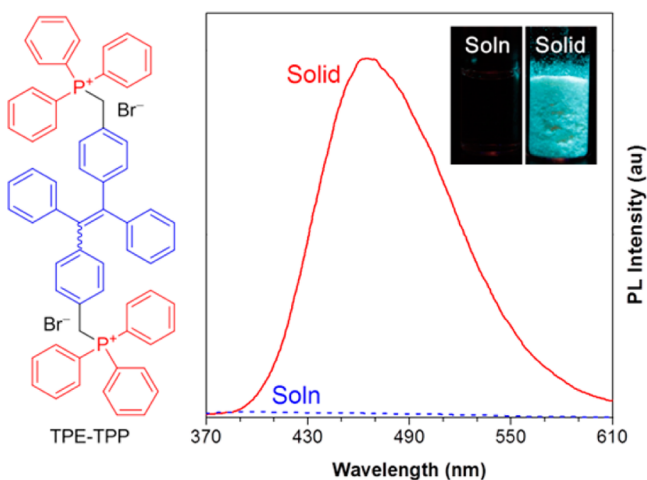


Figure 1. Chemical structure of TPE-TPP; PL spectra of TPE-TPP in solid and solution (soln) states. Inset: Photographs of DMF solution (left) and solid powder (right) of TPE-TPP taken under UV irradiation. Concentration of TPE-TPP: 10 μM ; excitation wavelength: 321 nm.

and the subsequent reaction with triphenylphosphine. The product was characterized by NMR and MS, and both gave satisfactory analysis data corresponding to their molecular structure (Figures S1–S3). Although carrying positive charges, TPE-TPP has relatively poor solubility in aqueous solution but is completely soluble in polar solvents, such as DMF and DMSO.

TPE-TPP shows typical AIE features, as shown in Figure 1. The DMF solution of TPE-TPP was almost nonemissive, while the solid state is strongly luminescent at 466 nm. Particle size analysis reveals the existence of particles with average size of 144 nm in aqueous solution containing 0.1% DMSO, the identical condition for cell staining, confirming that the TPE-TPP molecules have indeed formed aggregates in nanoscale (Figure S4).

Before the application for cell imaging, the cytotoxicity of TPE-TPP was evaluated using a 3-(4,5-dimethyl-2-thiazolyl)-2,5-diphenyltetrazolium bromide (MTT) assay (Figure S5). The result shows that the cell viability is not significantly altered when up to 7.5 μM TPE-TPP is added to the culture medium. TPE-TPP was then assessed for its ability to localize and stain mitochondria in living cells by fluorescence microscope. Cervical cancer HeLa cells were incubated with 5 μM TPE-TPP for 1 h, and excess dyes were washed away by buffer solution. As shown in Figure 2A, TPE-TPP stains specifically the mitochondrial region in HeLa cells. The reticulum structures of mitochondria are clearly visible with the aid of the blue fluorescence of TPE-TPP. The costaining

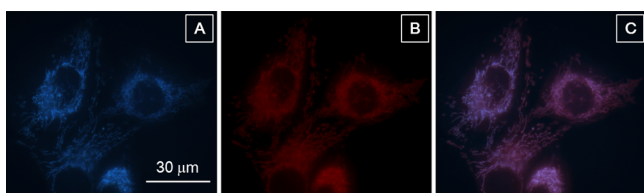


Figure 2. Fluorescent images of HeLa cells stained with (A) TPE-TPP (5 μM) for 1 h and (B) MitoTracker red FM (MT, 50 nM) for 15 min. (C) Panels A and B merged. Excitation wavelength: 330–385 nm (for TPE-TPP) and 540–580 nm (for MT).

experiment with MitoTracker red FM (MT), a commercially available mitochondria imaging agent,^{15,16} suggests that the observed fluorescence from TPE-TPP is localized to the mitochondria of the living HeLa cells (Figure 2). Pearson's correlation coefficient (R_r ; from +1 to -1), indicating the degree of linear dependence between two variables, is used to quantify the staining region overlap between TPE-TPP and MT. Fluorescence signals of the two dyes collected from two different channels are perfectly overlapped with $R_r = 0.96$, demonstrating the specific targeting of TPE-TPP on mitochondria. In Figure 2A, cells were incubated with TPE-TPP for 1 h. However, staining time as short as 15 min is sufficient for TPE-TPP to enter and light up mitochondria in cells (data not shown). Incubation time between 30 min to 2 h gives similar high signal-to-noise ratio (Figure S6).

The working concentrations of TPE-TPP and MT in our experiments were 5 μM and 50 nM, respectively. At first glance, one may think that MT is more sensitive than TPE-TPP. In a sense, it is true. But MT has a disadvantage at such low concentration because the dye molecules can be easily photobleached by the strong excitation light especially in confocal microscopes. At higher concentrations, these probes tend to lose the specificity and stain other cellular structures.¹⁷

Photostability is one of the most important criteria for developing fluorescent imaging agents. Continuous scanning by confocal microscope (Zeiss laser scanning confocal microscope LSM7 DUO) was used to quantitatively investigate the photostability of TPE-TPP and MT. Two dishes of HeLa cells subcultured from the same source were stained with 5 μM TPE-TPP for 1 h and 50 nM MT for 30 min, respectively. With the help of a power meter, excitation power from 405 and 560 nm channels of the microscope were unified (65 μW) and used to irradiate the TPE-TPP and MT stained cells. The initial intensity referred to the first scan of TPE-TPP and MT stained cells was normalized, and the percentage of fluorescence signal loss was calculated. As shown in Figure 3, during 50 scans with total irradiation time of ~ 7 min, the signal loss of TPE-TPP is less than 20%, and no significant difference was observed between the first and the 50th scan (video 1). Since live cells are dynamic, the movements of cells may attribute to the slight

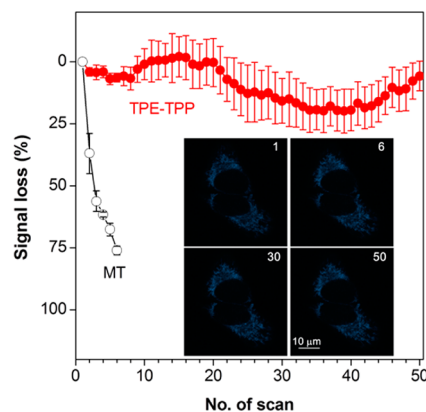


Figure 3. Signal loss (%) of fluorescent emission of TPE-TPP (solid circle) and MT (open circle) with increasing number of scans. Inset: fluorescent images of living HeLa cells stained with TPE-TPP (5 μM) with increasing number of scans (1–50 scans; the number of scans shown in upper right corner). Excitation wavelength: 405 nm (for TPE-TPP) and 560 nm (for MT); emission filter: 449–520 nm (for TPE-TPP) and 581–688 nm (for MT); irradiation time: 7.75 s/scan.

fluctuation of the signals. In contrast, the fluorescence signals of MT almost disappear after only 6 scans with <25% signal intensity remaining (video 2; Figure S7).

The formation of nanoaggregates of TPE-TPP when dispersed in aqueous media may facilitate the dye to diffuse across the cell membrane to accumulate in the mitochondrial region. Due to the AIE feature, the nanoaggregates of TPE-TPP are much brighter emitters than its single molecular form because the condensed packing in the aggregate state constrains the intramolecular motions and blocks the nonradiative decay channels.¹² When exposed to excitation light, the outermost layer of the nanoaggregates may be photobleached. However, the condensed particles can prevent further photobleaching and photo-oxidation by avoiding oxygen diffusion into the particles. For MT, unfortunately the working concentration is so low that even when accumulated in the mitochondrial matrix, it presents as an individual molecule which will be destroyed with ease by the strong excitation light.

Mitochondria are the organelles where cellular respiration occurs. Mitochondria continuously oxidize substrates and maintain a proton gradient across the lipid bilayer with very large membrane potential ($\Delta\Psi_m$) of around -180 mV.¹⁸ This value is double the plasma membrane of excitable cells and about six times larger than nonexcitable cell plasma membranes. Due to this large membrane potential gradient, mitochondria drive cationic species, such as TPP, into the matrix.¹⁹ As a result, their accumulation in mitochondria is 100–500-fold higher than in other parts of the cell. To test the tolerance of TPE-TPP and MT to the change of mitochondrial $\Delta\Psi_m$, carbonyl cyanide *m*-chlorophenylhydrazone (CCCP) was used to treat the cells prior to the staining procedure. CCCP is an uncoupler that causes rapid acidification of the mitochondria and dysfunction of ATP synthase resulting in the decrease of the mitochondrial $\Delta\Psi_m$.²⁰ Upon treatment with $20\ \mu\text{M}$ CCCP, the pH of mitochondria will decrease about 0.7,²¹ and $\Delta\Psi_m$ will thus decrease around 40 mV according to Nernst equation. When the cells were treated with $10\ \mu\text{M}$ CCCP, MT had no more specificity to mitochondria, and the sensitivity became worse (Figure 4A). Since the targeting of MT to mitochondria

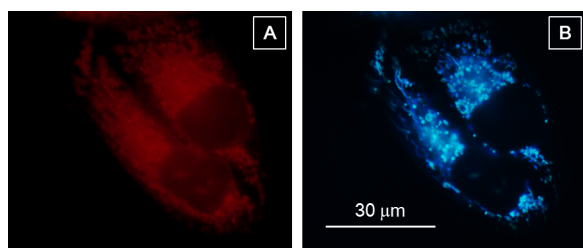


Figure 4. Fluorescent images of CCCP ($10\ \mu\text{M}$) treated HeLa cells stained with (A) MT ($50\ \text{nM}$) for 15 min and (B) TPE-TPP ($5\ \mu\text{M}$) for 30 min. Excitation wavelength: 540–580 nm (for MT) and 330–385 nm (for TPE-TPP).

is driven by the huge $\Delta\Psi_m$, the decrease of $\Delta\Psi_m$ will affect the direction and accumulation of cationic MT to mitochondria. It was expected that similar phenomena would be observed for TPE-TPP as it shares a similar working principle. Surprisingly, under the same condition, the specificity and sensitivity of TPE-TPP to mitochondria are perfectly retained in CCCP-treated cells (Figure 4B).

Compared with MT, TPE-TPP carries two positive charges, which allows a wider dynamic range for mitochondrial

targeting upon the change of $\Delta\Psi_m$. The lipophilicity may also play an important role in retaining the specificity and sensitivity of TPE-TPP in CCCP-treated HeLa cells. The lipophilicity of TPE-TPP is greatly enhanced by the TPE core with four phenyl rings rationalizing this phenomenon. On the other hand, MT carries only one positive charge (structure shown in Figure S8), and its selectivity is too susceptible to subtle change of $\Delta\Psi_m$ in mitochondria.

The high tolerance of TPE-TPP to the decrease of $\Delta\Psi_m$ enables the observation of change in mitochondrial morphology induced by CCCP (video 3).²² Upon exposure to CCCP, the reticulum-like mitochondria are gradually transformed to small and dispersed fragments (Figure 5). The early stage of

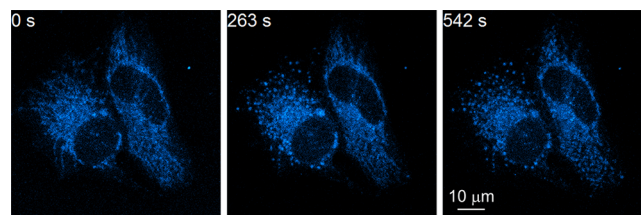


Figure 5. Fluorescent images of CCCP ($20\ \mu\text{M}$) treated living HeLa cells stained with TPE-TPP ($5\ \mu\text{M}$) with increasing scan time (the scan time shown in the upper left corner of the panel). Excitation wavelength: 405 nm; emission filter: 449–520 nm; irradiation time: 15.49 s/scan.

apoptosis involves remodeling of mitochondrial cristae and the consequent occurrence of morphological change of mitochondria, which is considered an irreversible process associated with the collapse of $\Delta\Psi_m$.⁷ TPE-TPP has excellent specificity to mitochondria with outstanding photostability and tolerance to microenvironment change, representing a potential candidate of tracking agent for apoptosis studies.

In conclusion, an AIE-active TPE derivative, TPE-TPP, has been synthesized and utilized as a fluorescent agent for mitochondrial imaging. Possessing high specificity to mitochondria, superior photostability, and appreciable tolerance to microenvironment change, TPE-TPP is a well-suited imaging agent for mitochondrial targeting and morphological change tracking. Because of its synthetic accessibility, TPE-TPP can be further modified as a dual-functional probe for an array of applications, such as sensing of ROS, metal ions, or pH change in mitochondria. Further studies on the development of AIE materials with different emission colors for organelles imaging and their biomedical applications are ongoing in our laboratories.

■ ASSOCIATED CONTENT

📄 Supporting Information

Experimental details and characterization data. The material is available free of charge via the Internet at <http://pubs.acs.org>

■ AUTHOR INFORMATION

Corresponding Author

tangbenz@ust.hk

Author Contributions

#These authors contributed equally.

Notes

The authors declare no competing financial interest.

■ ACKNOWLEDGMENTS

This work was partially supported by the Research Grants Council of Hong Kong (604711, 602212, HKUST2/CRF/10, and N_HKUST620/11), the University Grants Committee of Hong Kong (AoE/P-03/08), HKUST (RPC10SC13, RPC11SC09, and SRFI11SC03PG), the Innovation and Technology Commission (ITCPD/17-9), and the National Science Foundation of China (20974028). B.Z.T. thanks the support from Guangdong Innovative Research Team Program of China (201101C0105067115).

■ REFERENCES

- (1) Ow, Y.-L. P.; Green, D. R.; Hao, Z.; Mak, T. W. *Nat. Rev. Mol. Cell Biol.* **2008**, *9*, 532.
- (2) Hoye, A. T.; Davoren, J. E.; Wipf, P.; Fink, M. P.; Kagan, V. E. *Acc. Chem. Res.* **2008**, *41*, 87.
- (3) Dickinson, B. C.; Srikun, D.; Chang, C. J. *Curr. Opin. Chem. Biol.* **2010**, *14*, 50.
- (4) Dickinson, B. C.; Chang, C. J. *J. Am. Chem. Soc.* **2008**, *130*, 9638.
- (5) Karbowski, M.; Youle, R. J. *Cell Death Differ.* **2003**, *10*, 870.
- (6) Masanta, G.; Heo, C. H.; Lim, C. S.; Bae, S. K.; Cho, B. R.; Kim, H. M. *Chem. Commun.* **2012**, *48*, 3518.
- (7) Karbowski, M.; Youle, R. J. *Cell Death Differ.* **2003**, *10*, 870.
- (8) Gandre-Babbe, S.; van der Bliek, A. M. *Mol. Biol. Cell* **2008**, *19*, 2402.
- (9) Miyake, T.; McDermott, J. C.; Gramolini, A. O. *PloS One* **2011**, *6*, e28628.
- (10) Neto, B. a. D.; Carvalho, P. H. P. R.; Santos, D. C. B. D.; Gatto, C. C.; Ramos, L. M.; Vasconcelos, N. M. D.; Corrêa, J. R.; Costa, M. B.; de Oliveira, H. C. B.; Silva, R. G. *RSC Adv.* **2012**, *2*, 1524.
- (11) Hong, Y.; Lam, J. W. Y.; Tang, B. Z. *Chem. Commun.* **2009**, 4332.
- (12) Hong, Y.; Lam, J. W. Y.; Tang, B. Z. *Chem. Soc. Rev.* **2011**, *40*, 5361.
- (13) Chen, S.; Liu, J.; Liu, Y.; Su, H.; Hong, Y.; Jim, C. K. W.; Kwok, R. T. K.; Zhao, N.; Qin, W.; Lam, J. W. Y.; Wong, K. S.; Tang, B. Z.; Wong, S. *Chem. Sci.* **2012**, *3*, 1804.
- (14) Yu, Y.; Feng, C.; Hong, Y.; Liu, J.; Chen, S.; Ng, K. M.; Luo, K. Q.; Tang, B. Z. *Adv. Mater.* **2011**, *23*, 3298.
- (15) Dong, L.-F.; Jameson, V. J. a.; Tilly, D.; Prochazka, L.; Rohlena, J.; Valis, K.; Truksa, J.; Zabalova, R.; Mahdavian, E.; Kluckova, K.; Stantic, M.; Stursa, J.; Freeman, R.; Witting, P. K.; Norberg, E.; Goodwin, J.; Salvatore, B. a.; Novotna, J.; Turanek, J.; Ledvina, M.; Hozak, P.; Zhivotovsky, B.; Coster, M. J.; Ralph, S. J.; Smith, R. a J.; Neuzil, J. *Free Radical Biol. Med.* **2011**, *50*, 1546.
- (16) Yang, G.; Liu, L.; Yang, Q.; Lv, F.; Wang, S. *Adv. Funct. Mater.* **2012**, *22*, 736.
- (17) Johnson, I.; Ph, D.; Spence, M. T. Z.; Walker, C.; Buller, G.; Asp, M. T.; Croissant, J. *The Molecular Probes Handbook editors scientific support Graphics Production and layout*, 11th ed.; Life Technologies Corporation: Carlsbad, CA, 2010.
- (18) Casey, J. R.; Grinstein, S.; Orłowski, J. *Nat. Rev. Mol. Cell Biol.* **2010**, *11*, 50.
- (19) Murphy, M. P. *Biochim. Biophys. Acta* **2008**, *1777*, 1028.
- (20) de Graaf, A. O.; van den Heuvel, L. P.; Dijkman, H. B. P. M.; de Abreu, R. a; Birkenkamp, K. U.; de Witte, T.; van der Reijden, B. a; Smeitink, J. a M.; Jansen, J. H. *Exp. Cell Res.* **2004**, *299*, 533.
- (21) Takahashi, A.; Centonze, V. E.; Herman, B. *BioTechniques* **2001**, *30*, 804.
- (22) Gottlieb, E.; Armour, S. M.; Harris, M. H.; Thompson, C. B. *Cell Death Differ.* **2003**, *10*, 709.